

Optimization of organic bi-layer solar cell through systematic study of anode treatment and material thickness

Young Wook Kim*, Matthew L. Monroe**, Jiyoun Seol*, Nguyen Tam Nguyen Truong*, Sung Min Cho***, Timothy J. Anderson**, and Chinho Park*[†]

*School of Display and Chemical Engineering, Yeungnam University, Gyeongsan 712-749, Korea

**Department of Chemical Engineering, University of Florida, Gainesville FL 32611, USA

***Department of Chemical Engineering, Sungkyunkwan University, Suwon 440-746, Korea

(Received 2 August 2007 • accepted 6 March 2008)

Abstract—The performance of bi-layer organic solar cells with the structure ITO/PEDOT:PSS/CuPc/C₆₀/BCP/Al was optimized. Prior to cell deposition, an optimal indium tin oxide (ITO) surface treatment technique was determined, with N₂ plasma treatment providing the highest solar cell efficiency. Parametric studies were performed to identify optimal fabrication conditions and deposition thicknesses for each layer by using solar cell efficiency as the primary performance measure.

Key words: Organic Solar Cell, Bi-layer Solar Cell, Plasma Treatment, Deposition Thickness, Optimization

INTRODUCTION

Recently, organic semiconductor devices have increasingly penetrated markets traditionally held by inorganic semiconductor devices in fields such as light emitting diodes, field effect transistors, photodetectors and solar cells. It is well known that some organic materials demonstrate a strong photoelectric effect, making them suitable materials for solar cells. The first organic thin film solar cells, which were constructed in 1958, suffered from short lifetimes and low efficiencies compared to inorganic cells being developed. Despite these challenges, organic photovoltaics have grown into a broad research field. This is primarily due to their key advantages such as flexibility, light weight, and low production costs [1,2].

With the ongoing worldwide push toward renewable energy, organic solar cells continue to show strong promise as sources of significant energy production in the near future [3,4]. The development of crystalline organic materials with high doping levels, as well as advances in cell structures such as donor-acceptor hetero-junctions, blended junctions, and exciton blocking layers have driven a continuous increase in organic cell efficiencies [5].

This manuscript is focused on optimization of the fabrication process for organic bi-layer solar cells. Cell efficiency has reached 3.6% in these cells, but further increases have been limited by low electron mobility [6]. This study attempts to improve organic bi-layer solar cell performance through two methods. The first method is the development of an optimal surface treatment technique for the indium tin oxide (ITO) anode. ITO surface treatment has previously demonstrated improvements in organic light-emitting diode (OLED) performance. In case of an OLED, an increase in anode work function following treatment by O₂ plasma improved carrier injection into the organic layers [7]. On the other hand, the solar cell anode should be shifted to a lower work function because the goal is charge extraction rather than charge injection. The second performance

enhancement technique is the layer-by-layer optimization of the cell structure to optimize the balance between photon absorption and charge transport. To quantify the effect of these studies, organic bi-layer solar cells with the basic structure of contact electrode/hole transporter/light absorber/electron transporter/exciton blocker/contact electrode were fabricated and the device performance measured.

EXPERIMENTAL

Organic bi-layer solar cells were built on glass substrates with a 1,800 Å ITO film and a sheet resistance of approximately 7 Ω/sq. The commercially available substrates were cleaned by using a three-step process of sequential ultrasonification in trichloroethylene, acetone, and methanol, and were then dried under nitrogen. Some ITO surfaces were then subjected to one of three treatment procedures: exposure to nitrogen plasma, exposure to oxygen plasma, or exposure to an electron beam under a nitrogen atmosphere. The anode surface was characterized with x-ray photoelectron spectroscopy (XPS), atomic force microscopy (AFM), and a video contact angle system (VCAS) to determine the effect of the treatments.

For cell fabrication, a hole-transport layer (HTL) of poly-ethylene di-oxythiophene:poly-styrenesulfonate (PEDOT : PSS) was deposited through spin-coating and dried in a vacuum oven. The active layer of copper phthalocyanine (CuPc), electron transport layer (ETL) of C₆₀, exciton blocking layer (EBL) of bathrocuproine (BCP), and back aluminum contact were deposited at room temperature in a thermal evaporator with a base pressure of 1.2 × 10⁻⁶ Torr. The solar cell efficiency was measured in the dark and under illumination from a solar simulator set to produce an AM 1.5 100 mW/cm² light.

RESULTS AND DISCUSSION

ITO surface treatment was performed by exposing the sample to N₂ plasma, O₂ plasma, or electron beam. After treatment, the surface energy, surface roughness, and work function were measured. Fig. 1 shows a test of the ITO surface energy by using a VCAS. In

*To whom correspondence should be addressed.

E-mail: chpark@ynu.ac.kr

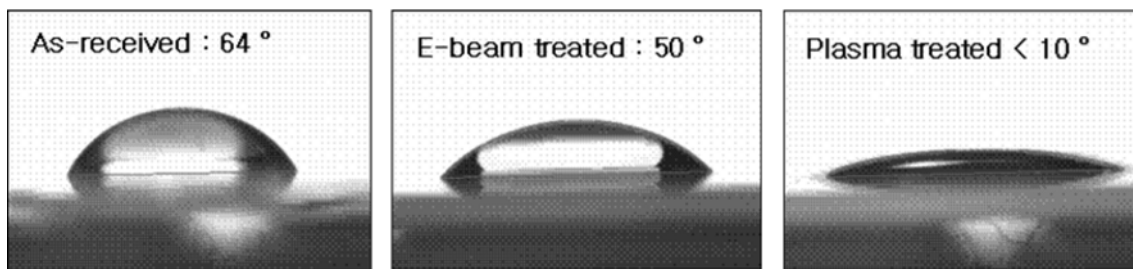


Fig. 1. Contact angle of a water droplet on bare and treated ITO surfaces recorded by a video contact angle system. A lower contact angle corresponds to higher surface energy.

In this experiment, a small drop of water is placed on the film surface and the contact angle between the drop edge and the film is measured, with a smaller contact angle signifying higher film energy. Since the PEDOT:PSS solution used as the HTL for these cells uses water as a solvent, this test can be used to directly compare the wetting nature and therefore predict the quality of films deposited on these ITO substrates. As shown in Fig. 1, treatment with either N₂ or O₂ plasma resulted in a contact angle of less than 10 degrees. It is obvious from the test that O₂ and N₂ plasma treatments provide a much more energetic surface, which results in a very low contact angle and the potential to deposit high-quality films.

The surface roughness of ITO films was studied with AFM before and after surface treatment. As shown in Fig. 2, the ITO films

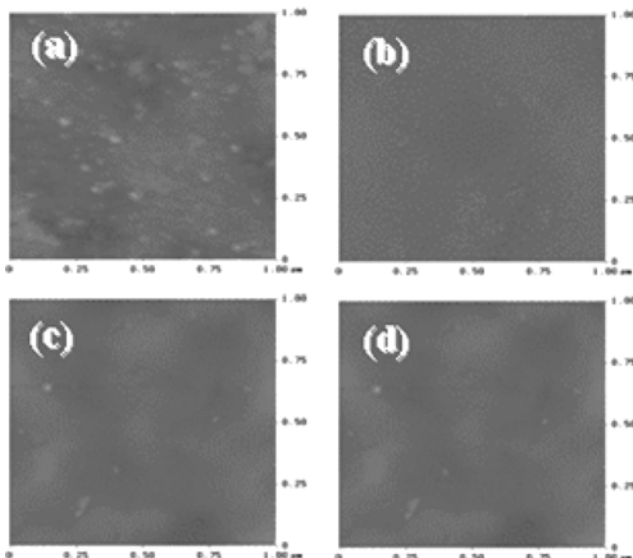


Fig. 2. RMS surface roughness of bare and treated ITO surfaces measured by AFM: (a) As-received: 1.049 nm, (b) E-beam: 0.774 nm, (c) O₂ plasma: 0.823 nm, (d) N₂ plasma: 0.614 nm.

show a much smoother surface after N₂ plasma treatment compared to surfaces after O₂ plasma or e-beam treatment. ITO surface roughness impacts the roughness of subsequent cell layers, which effects charge mobility in the cell and therefore impacts the cell efficiency.

XPS was used to study the change in the surface composition of the ITO films after exposure to a treatment. From the results shown in Table 1, E-beam treatment does not significantly alter the ITO surface composition, so its impact on device performance is anticipated to be minimal. On the contrary, after N₂ plasma treatment the In/Sn ratio of the film surface decreased and the number of electrons at the ITO surface increased [8,9]. The Fermi energy of N₂ plasma treated ITO increased, and the film work function decreased [10]. This results from the formation of InN from the reaction of nitrogen radicals and surface indium atoms, with this new material subsequently being removed from the film.

Organic bi-layer solar cells were fabricated on substrates sub-

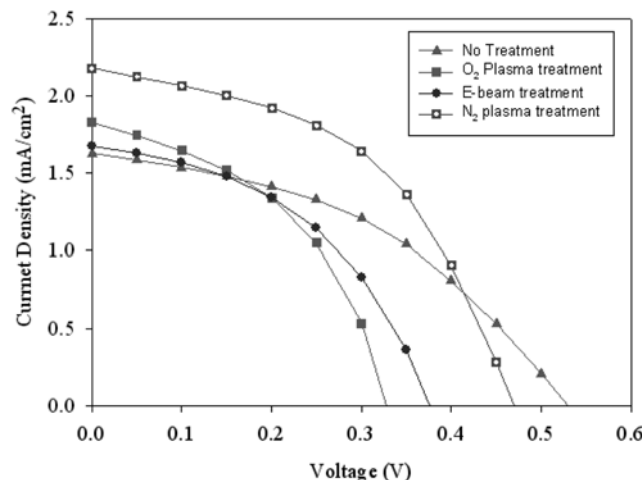


Fig. 3. J-V curves of solar cells deposited on treated ITO substrates.

Table 1. Chemical composition of ITO films measured by XPS

Condition	Atomic composition				Atomic ratio	
	O	Sn	In	N	O/In	In/Sn
No treatment	0.5675	0.0265	0.406	-	1.397	15.32
After N ₂ plasma treatment (50 W, 1 Torr, 10 min)	0.5549	0.0267	0.4049	0.0135	1.37	15.16
After e-beam treatment (2 KGy)	0.5667	0.0238	0.3876	0.0219	1.462	16.28

jected to these treatment techniques. Fig. 3 shows that O₂ plasma and e-beam treated substrates showed lower device efficiency than untreated substrates, while N₂ plasma treated substrates showed increased efficiency. The smoother surface, improved chemical stability, and reduced work function after N₂ plasma treatment combine to grant this performance increase [8,9].

Using N₂ plasma exposure for anode treatment, bi-layer solar cell optimization was performed by systematically varying the thickness of each layer to maximize cell efficiency. CuPc was chosen as the p-type active layer material in the bi-layer solar cell and was deposited by thermal evaporation. The deposition occurred at a constant rate, with film thickness controlled by varying the deposition time. The C₆₀ ETL thickness was fixed at 10 nm for these studies. As seen in Fig. 4, the optimal film thickness was 26 nm. At slightly larger thicknesses, the efficiency is only slightly improved due to a low built-in electric field from the relatively thin C₆₀ electron acceptor layer. Slightly smaller thicknesses, however, result in a significant efficiency drop due to limitations to photon absorption.

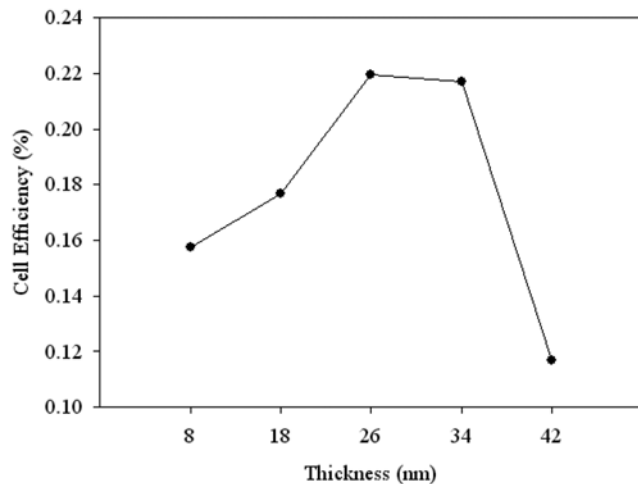


Fig. 4. Optimization of CuPc thickness: C₆₀ thickness was fixed at 10 nm.

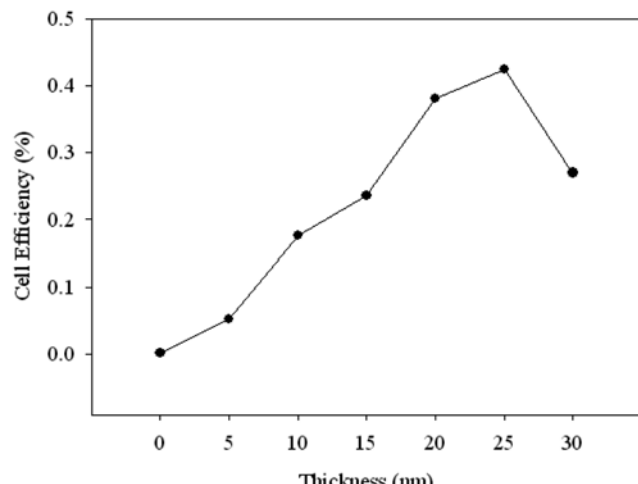


Fig. 5. Optimization of C₆₀ thickness: CuPc thickness was fixed at 26 nm.

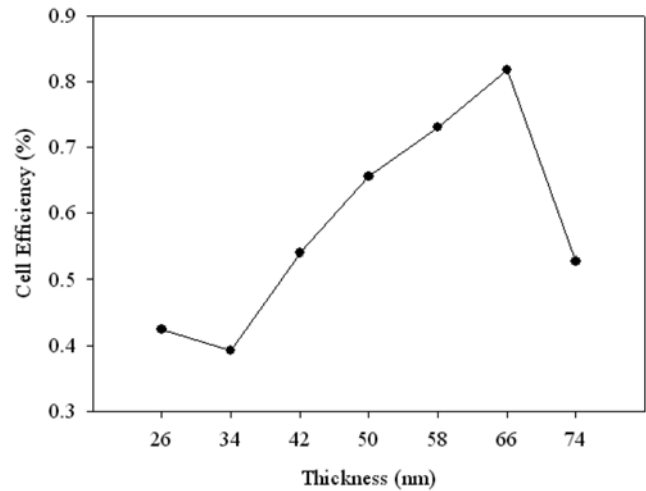


Fig. 6. Optimization of CuPc thickness: C₆₀ thickness was fixed at 25 nm.

After the CuPc thickness was fixed at 26 nm, the C₆₀ thickness was varied from 0 to 30 nm to optimize charge separation and transport. As shown in Fig. 5, the device efficiency was very low when no C₆₀ was present in the cell. This is because excitons generated in the CuPc film did not have an active interface to allow dissociation, so they simply recombined. As the C₆₀ layer thickness increased, device efficiency improved, because as the thickness of the electron acceptor increased, the excitons were more easily separated into free carriers. This improvement continued up to 25 nm. After that point, the device efficiency dropped due to increased series resistance.

With the electron acceptor thickness now set at the optimal value of 25 nm, the electron donor thickness was varied around the previous setpoint of 26 nm. Fig. 6 shows that as the CuPc thickness increased up to 66 nm, cell efficiency improved. Since CuPc is the primary absorbing material, an increase in the CuPc thickness results in more light absorbed in the cell, generating more excitons. In combination with the optimized C₆₀ layer, this increased the amount of free carriers that could be generated in the cell. Further thickness increases of this layer resulted in a strong drop in current through the devices. This is attributed to a limitation in the exciton diffusion length. As the CuPc thickness increases, a larger percentage of the excitons are unable to reach the interface before recombining, resulting in a loss of current in the cells. The HTL thickness of less than 20 nm showed significant drop in the cell efficiency primarily due to the current leakage paths developed by pin-holes.

PEDOT:PSS was chosen as the hole-transport layer (HTL). This film was deposited by spin-coating, and the thickness was varied by changing the spin-coating speed. Cell efficiency was found to improve as this layer was reduced to 20 nm, as illustrated in Fig. 7. The primary purposes of the HTL are to smooth the ITO surface and to provide an energy level for hole transport in the energy band diagram. This can be achieved with a thin layer, and any additional thickness only serves to increase series resistance to the current flow.

Finally, the exciton blocking layer (EBL) of BCP was included, which helps to prevent exciton recombination at the Al electrode. Because of the transparency of this film, it was difficult to accu-

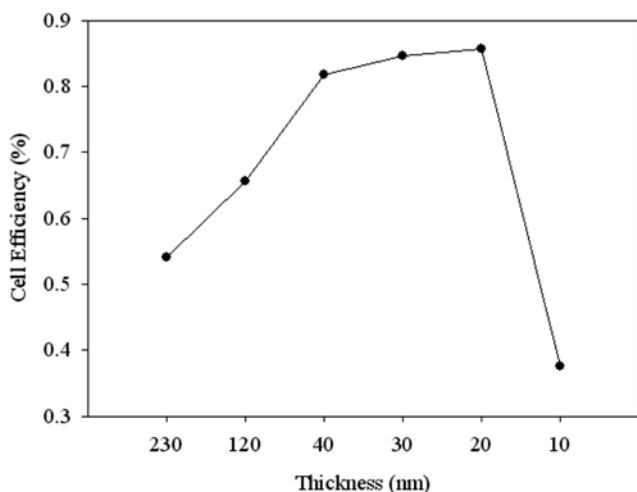


Fig. 7. Optimization of PEDOT:PSS thickness: CuPc thickness was fixed at 28 nm and C₆₀ thickness was fixed at 25 nm.

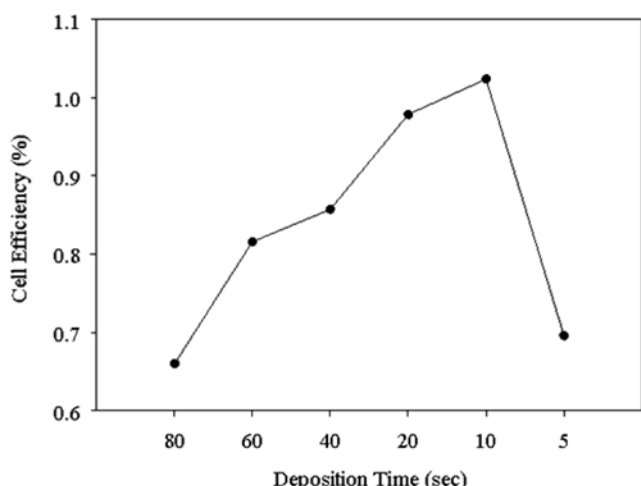


Fig. 8. Optimization of BCP thickness by controlling deposition time: Fixed layer thicknesses were 20 nm for PEDOT:PSS, 66 nm for CuPc, and 25 nm for C₆₀.

rately measure the film thickness, so it was estimated by accurately controlling the deposition time at a constant evaporation rate. BCP is a wide band-gap material whose purpose is to prevent holes and excitons from reaching the aluminum electrode, where they can impede the current flow. Fig. 8 demonstrates that thinner layers of BCP resulted in improved device efficiency due to reduced series resistance in the cell. Solar cell efficiency was improved until the BCP deposition time was decreased to 10 sec. After that point, however, the device efficiency dropped due to increased exciton recombination.

SUMMARY

Investigations have been performed to optimize the performance of ITO/PEDOT:PSS/CuPc/C₆₀/BCP/Al bi-layer solar cells. Due to improved cell performance, decreased surface roughness, enhanced surface energy due to incorporation of nitrogen into the ITO, and a decrease in the ITO work function, it was determined that N₂ plasma treatment is superior to O₂ plasma and electron beam treatment. Using this treatment technique under optimized conditions, the thickness of each layer was systematically varied to optimize the overall cell performance. The thickness of the absorber layer and ETL were increased to allow more complete absorption and increase the strength of the built-in field for charge collection, while the HTL and EBL films were thinned to reduce series resistance in the cells. The final optimized cell structure was ITO/PEDOT:PSS (20 nm)/CuPc (66 nm)/C₆₀ (25 nm)/BCP/Al. The optimal deposition time for the BCP layer was 10 sec.

ACKNOWLEDGMENT

This work was supported by grant No. RTI04-01-04 from the Regional Technology Innovation Program of the Korean Ministry of Commerce, Industry, and Energy (MOCIE), and the researchers involved in this work were partially supported by the 2nd phase of the BK21 Program.

REFERENCES

1. P. A. Lane and Z. H. Kafafi, in *Organic photovoltaics mechanism, materials and device*, S. S. Sun and N. S. Sariciftci, Eds., Taylor & Francis, Florida (2005).
2. A. J. Heeger, *Rev. Mod. Phys.*, **73**, 681 (2001).
3. J. H. Schon, C. Kloc and B. Batlogg, *Appl. Phys. Lett.*, **77**, 2473 (2000).
4. G. Yu, J. Gao, J. C. Hummelen, F. Wudl and A. J. Heeger, *Science*, **270**, 1789 (1995).
5. B. Brousse, B. Ratier and A. Moliton, *Synth. Met.*, **147**, 293 (2004).
6. P. Peumans and S. R. Forrest, *Appl. Phys. Lett.*, **79**, 126 (2001).
7. H. Kim, J. Lee, T. Lee, J. Kim and H. Park, *Proceedings of the 1st International Meeting on Information Display*, 626 (2001).
8. J. Seol, M. L. Monroe, T. J. Anderson, M. A. Hasnain and C. Park, *Conference Record of the 2006 IEEE[®] World Conference on Photovoltaic Energy Conversion*, 236 (2006).
9. Y. W. Kim, M. L. Monroe, J. Seol, D. H. Kim, T. W. Koo, T. J. Anderson and C. Park, *Mater. Res. Soc. Symp. Proc.*, **1013**, Z07-21 (2007).
10. K. Sugiyama, H. Ishii and Y. Ouchi, *J. Appl. Phys.*, **87**, 295 (2000).